

An Overview On Equalization Techniques for MIMO-OFDM Systems

Negar Mohaghegh, Shima Kheradmand, and Nahid Ghofrani
Isfahan University of Technology

Abstract- In this paper, we overview the fundamental techniques of MIMO OFDM equalization in channels where the maximum delay exceeds the length of the Guard Interval. The paper is divided to three main parts explaining frequency domain, time domain and turbo equalization, respectively. In frequency domain, per-tone equalization was chosen to be explained. Swapping the filtering operations of MIMO channel and sliding FFT, one can use the same equalization method of MIMO SC for each tone of MIMO OFDM. In time domain, we discuss techniques in which second order statistics of received signal is used. It is proven that this method is much more efficient than other time domain techniques such as channel shortening. In last chapter we will explain using of Turbo equalization in MIMO OFDM systems which is an iterative equalization and decoding technique for suppressing ISI.

I. INTRODUCTION

In mobile communications, Orthogonal Frequency Division Multiplexing (OFDM) has attracted much attention because it can realize more reliable and higher data-rate transmission. OFDM achieves the ISI-free transmission in the frequency selective fading by the combination of the orthogonal multi carrier and the Guard Interval (GI). However, in the outdoor applications the delay difference between the first and the last delayed paths sometimes becomes greater than GI, and even the OFDM transmission suffers from severe degradation.

This excess delay causes both Inter-Symbol Interference (ISI) to the adjacent OFDM symbols and Inter-Carrier Interference (ICI) within the same symbol. This is why OFDM equalization techniques have been discussed so much in literature.

On the other hand one can not deny the effectiveness of multiple-input multiple-output (MIMO) systems in broadband communication. As a matter of fact, MIMO broadband systems based on spatial multiplexing techniques combined with orthogonal frequency division multiplexing (MIMO-OFDM) are seen as efficient key technologies for next generation wireless systems. In MIMO-OFDM, the receiver complexity is significantly reduced using the Fast Fourier Transform (FFT) to transmit data in parallel over a large number of sub-carriers and introducing a guard interval (GI) in every symbol. But just as a simple OFDM system, the MIMO one needs also to use channel equalization. This paper aims to review the principal techniques of channel equalization for MIMO-OFDM systems.

We put all variant techniques of equalization in three categories. The first one is frequency domain technique which includes per-tone equalization and will be discussed in chapter II. In receiver demodulating FFT is implemented as a sliding FFT, and then its output is downsampled. It can be shown that if filtering operations of the MIMO channel and the sliding FFT are swapped, because of the similarity of the obtained data model for the temporally smoothed received signal of each individual tone of the MIMO OFDM system to the data model for it's corresponding in MIMO SC system the same

equalization method for the latter can be used for each individual tone of the MIMO OFDM system.

The second technique is time domain equalization. Channel shortening and time domain statistics-based techniques are two different methods in time domain. Latter is discussed in chapter IV in details. In this algorithm i -th received OFDM block is left shifted by J samples, which is resulted in some useful structural properties to cancel most of the ISI using the second order statistics of the received signals before signal detection. In this technique channel length information is not needed and estimation of only $2D$ columns of the channel matrix with a minimum of $4D$ pilot symbols is sufficient with D to be the maximum channel length.

As third category, we have Turbo Equalization which is an iterative equalization and decoding technique. This method is one of the promising approaches to reduce interference especially when the excess delay is greater than one half of the symbol duration. In chapter V, we first discuss some basic ideas of Turbo Equalization without going through unnecessary details. Then we will conclude the most popular MIMO OFDM turbo equalizer in literature.

II. Per-Tone Equalization

A. Main Concept:

In this section, we focus on MIMO OFDM systems with channel order larger than the cyclic prefix (CP) length. Writing the demodulating fast Fourier transform (FFT) as a sliding FFT followed by a downsampling operation, we show that by swapping the filtering operations of the MIMO channel and the sliding FFT, the data model for the temporally smoothed received signal of each individual tone of the MIMO OFDM system is very similar to MIMO SC system. As a result, to recover the data symbol vectors, the conventional equalization approach for MIMO SC systems can be applied to each individual tone of the MIMO OFDM system [1]. This so-called per-tone equalization (PTEQ) approach for MIMO OFDM systems is an attractive alternative to the recently developed time-domain equalization (TEQ) approach for MIMO OFDM systems [2]. Comparing the PTEQ approach with the TEQ approach for MIMO OFDM systems leads to the following observations:

- Since the PTEQ approach treats all tones separately, whereas the TEQ approach treats all tones jointly, the PTEQ approach always has a better performance than the TEQ approach. In addition, the performance of the PTEQ approach is a much smoother function of the synchronization delay. Hence, for the PTEQ approach the synchronization delay setting is less critical.
- Since the PTEQ approach works at low rate in the frequency domain, whereas the TEQ approach works at high rate in the time-domain, the show-time complexities of the PTEQ approach and the TEQ approach are comparable, up to the fact that the PTEQ approach has to carry out one FFT per OFDM symbol and per receive

antenna, whereas the TEQ approach has to carry out one FFT per OFDM symbol and per transmit antenna.

- Since the PTEQ approach uses a different set of equalizer coefficients for each tone, whereas the TEQ approach uses the same set of equalizer coefficients for each tone, the PTEQ approach requires more memory space than the TEQ approach, and the design complexity of the PTEQ approach is generally larger than the design complexity of the TEQ approach.

Note that the PTEQ approach merely tries to equalize the MIMO channel, and any type of MIMO OFDM processing can be used on top of this equalization structure. In practice, the per-tone equalizers have to be designed. Focusing on direct per-tone equalizer design, one can basically adapt existing direct equalizer design methods for MIMO SC systems to the corresponding direct per-tone equalizer design methods for MIMO OFDM systems [3].

In Section II, we describe the data model of a MIMO OFDM system, briefly. In Section III, we present the PTEQ approach. In Section IV, we show simulation.

Notation: Upper (lower) bold face letters denote matrices (column vectors); frequency-domain components are indicated by a tilde; $(\cdot)^T$, $(\cdot)^H$, and $(\cdot)^+$ denote transpose, Hermitian, and pseudo-inverse, respectively; \otimes stands for the Kronecker product; $\|\cdot\|$ represents the Frobenius norm; and finally, $\mathbf{0}_{M \times N}$ and $\mathbf{1}_{M \times N}$ denote the $M \times N$ all-zero matrix and the $M \times N$ all-one matrix, respectively.

B. Data Model:

We consider a MIMO OFDM system with L_T transmit antennas and L_R receive antennas. Suppose the $L_T \times 1$ vector $\mathbf{z}_{i,p}$ represents the data symbol vector corresponding to the p -th tone of the i -th OFDM symbol ($p \in \{0, 1, \dots, N-1\}$). The $L_T \times 1$ vector that is transmitted over the L_T transmit antennas at time instant n can then be written as

$$\mathbf{z}_i[n] = \frac{1}{\sqrt{N}} \sum_{p=0}^{N-1} e^{j2\pi(q-G)p/N} \mathbf{z}_{i,p},$$

where $i = \lfloor n/(N+G) \rfloor$, and $q = n - i(N+G)$. G is the CP length. Performing a N -point FFT on the vector sequence $\mathbf{z}_i[(N+G)+G+\delta], \dots, \mathbf{z}_i[(N+G)+N-1+G+\delta]$, the vector $L_T \times 1$ corresponding to the p -th tone of the i -th OFDM symbol can be written as

$$\mathbf{z}_\delta^{(p)}[i] = \frac{1}{\sqrt{N}} \sum_{q=0}^{N-1} e^{-j2\pi pq/N} \mathbf{z}_i[(N+G)+q+G+\delta] = e^{j2\pi p\delta/N} \mathbf{z}_{i,p}$$

for $-G < \delta \leq 0$.

The vector $L_R \times 1$ that is received at the L_R receive antennas at time instant n is given by

$$\mathbf{r}_n = \sum_{d=0}^D \mathbf{H}_d \mathbf{z}_i[n-d] + \mathbf{e}_n$$

where \mathbf{H}_l is the $L_R \times L_T$ MIMO channel with order L , which is assumed to be larger than G . Considering the $(K+1)L_R \times 1$ vector obtained after temporally smoothing \mathbf{r}_n

$$\mathbf{r}_{n-K:n} := [\mathbf{r}_{n-K}^T, \dots, \mathbf{r}_n^T]^T$$

we obtain

$$\mathbf{r}_{n-K:n} = \hat{\mathbf{H}} \mathbf{z}_{n-K-L:n} + \mathbf{n}_{n-K:n}$$

Where $\mathbf{n}_{n-K:n}$ and $\mathbf{z}_{n-K-L:n}$ are similarly defined as $\mathbf{r}_{n-K:n}$, and $\hat{\mathbf{H}}$ is the $(K+1)L_R \times (K+L+1)L_T$ block Toeplitz matrix given by

$$\hat{\mathbf{H}} := \begin{bmatrix} \mathbf{H}_L & \mathbf{H}_{L-1} & \cdots & \mathbf{H}_0 \\ & \mathbf{H}_L & \mathbf{H}_{L-1} & \cdots & \mathbf{H}_0 \\ & & \ddots & & \\ & & & \mathbf{H}_L & \mathbf{H}_{L-1} & \cdots & \mathbf{H}_0 \end{bmatrix}$$

Performing a N -point FFT on the vector sequence $\mathbf{r}_{i(N+G)+G+\delta}, \dots, \mathbf{r}_{i(N+G)+N-1+G+\delta}$, the $L_R \times 1$ vector corresponding to the p -th tone of the i -th OFDM symbol can be written as:

$$\mathbf{r}_\delta^{(p)}[i] = \frac{1}{\sqrt{N}} \sum_{q=0}^{N-1} e^{-j2\pi pq/N} \mathbf{r}_{i(N+G)+q+G+\delta}$$

If we now plug in (3), swap the filtering operations of the MIMO channel and the sliding FFT, and use (2), we obtain

$$\mathbf{r}_\delta^{(p)}[i] = \sum_{l=0}^L \mathbf{H}_l \mathbf{z}_{\delta-l}^{(p)}[i] + \mathbf{n}_\delta^{(p)}[i]$$

Where $\mathbf{n}_\delta^{(p)}[i]$ is similarly defined as $\mathbf{r}_\delta^{(p)}[i]$. Considering the $(K+1)L_R \times 1$ vector $\mathbf{r}_{\delta-K:\delta}^{(p)}[i]$ obtained after temporally smoothing $\mathbf{r}_\delta^{(p)}[i]$, we obtain

$$\mathbf{r}_{\delta-K:\delta}^{(p)}[i] = \hat{\mathbf{H}} \mathbf{z}_{\delta-K-L:\delta}^{(p)}[i] + \mathbf{n}_{\delta-K:\delta}^{(p)}[i]$$

Where $\mathbf{n}_{\delta-K:\delta}^{(p)}[i]$ and $\mathbf{z}_{\delta-K-L:\delta}^{(p)}[i]$ is similarly defined as $\mathbf{r}_{\delta-K:\delta}^{(p)}[i]$.

Assuming that $0 \leq \delta \leq K+L-G$, we can last equation as:

$$\mathbf{r}_{\delta-K:\delta}^{(p)}[i] = \hat{\mathbf{H}}_\delta^{(p)} \mathbf{z}_{\delta-K-L:\delta}^{(p)}[i] + \mathbf{n}_{\delta-K:\delta}^{(p)}[i]$$

Where $\mathbf{z}_{\delta-K-L:\delta}^{(p)}[i] := [\mathbf{z}_{\delta-K-L:-G-1}^{(p)T}[i], \mathbf{z}_{\delta-K-L}^{(p)T}[i], \mathbf{z}_{\delta-K}^{(p)T}[i]]^T$, and

$$\hat{\mathbf{H}}_\delta^{(p)} := \hat{\mathbf{H}} \begin{bmatrix} \mathbf{I}_{(K+L-\delta-G)L_T} & & \\ & \mathbf{d}^{(p)} \otimes \mathbf{I}_{L_T} & \\ & & \mathbf{I}_{\delta L_T} \end{bmatrix}$$

with $\mathbf{d}^{(p)} := [e^{-j2\pi pG/P}, \dots, e^{-j2\pi p/P}]^T$.

The above data is very similar to the data model for the tempo-rally smoothed received signal of a MIMO SC system [4]. The difference is that the channel matrix is a column-compressed block Toeplitz matrix with $(L+K-G+1)L_T$ columns instead of a block

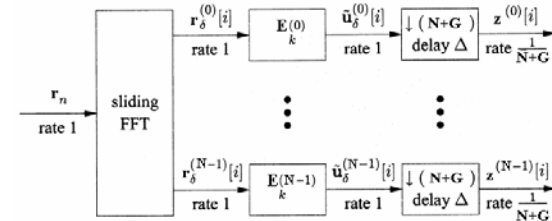


Fig. 1. Block diagram of the PTEQ approach.

Toeplitz matrix with $(L+K+1)L_T$ columns, and the ISI consists of $L+K-G$ virtual data symbol vectors instead of

$L + K$ true data symbol vectors. However, since the conventional equalization approach for MIMO SC systems requires neither the channel matrix to be block Toeplitz nor the ISI to consist of true data symbol vectors, we can apply the conventional equalization approach for MIMO SC systems to the p -th tone of the MIMO OFDM system in order to recover $\mathbf{z}_{i,p}$.

C. PTEQ Approach:

In the PTEQ approach, which is depicted in Fig. 1, we apply an $L_T \times L_R$ per-tone equalizer $\mathbf{E}_k^{(p)}$ with order K to $\tilde{\mathbf{y}}_\delta^{(p)}[i]$

$$\hat{\mathbf{z}}_{i,p} = \tilde{\mathbf{u}}_\delta^{(p)}[i] = \sum_{k=0}^K \mathbf{E}_k^{(p)} \mathbf{r}_{\delta-K}^{(p)}[i]$$

The goal of the per-tone equalizer $\mathbf{E}_k^{(p)}$ is to find an estimate of $\mathbf{z}_{i,p}$ from $\tilde{\mathbf{u}}_\delta^{(p)}[i]$ evaluated at $\delta = \Delta$ (Δ is called the synchronization delay). This equation can be rewritten as

$$\hat{\mathbf{z}}_{i,p} := \mathbf{E}^{(p)} \mathbf{r}_{\Delta-K:\Delta}^{(p)}[i]$$

where $\mathbf{E}^{(p)} := [\mathbf{E}_1^{(p)}, \dots, \mathbf{E}_{L_T}^{(p)}]$. Assuming $0 \leq \Delta \leq K + L - G$,

we can obtain $\mathbf{r}_{\delta-K:\delta}^{(p)}[i]$ using previous equations.

We can adopt the zero-forcing (ZF) per-tone equalizer, which is given by

$$\mathbf{E}_{ZF}^{(p)} = \mathbf{S} (\hat{\mathbf{H}}_\Delta^{(p)H} \mathbf{R}_{\mathbf{e}_{\Delta-K:\Delta}}^{(p)-1} \hat{\mathbf{H}}_\Delta^{(p)})^{-1} \hat{\mathbf{H}}_\Delta^{(p)H} \mathbf{R}_{\mathbf{e}_{\Delta-K:\Delta}}^{(p)-1}$$

or the minimum mean-square error (MMSE) per-tone equalizer, which is given by

$$\mathbf{E}_{MMSE}^{(p)} := \mathbf{S} (\hat{\mathbf{H}}_\Delta^{(p)H} \mathbf{R}_{\mathbf{e}_{\Delta-K:\Delta}}^{(p)-1} \hat{\mathbf{H}}_\Delta^{(p)} + \mathbf{R}_{\mathbf{e}_{\Delta-K-L:\Delta}}^{(p)-1})^{-1} \times \hat{\mathbf{H}}_\Delta^{(p)H} \mathbf{R}_{\mathbf{e}_{\Delta-K:\Delta}}^{(p)-1}$$

where \mathbf{S} is the $L_T \times (L + K - G + 1)L_T$ matrix defined as

$$\mathbf{S} := [\mathbf{0}_{L_T \times (L+K-G-\Delta)L_T}, \mathbf{I}_{L_T}, \mathbf{0}_{L_T \times \Delta L_T}]$$

$\mathbf{R}_{\mathbf{e}_{\Delta-K:\Delta}}^{(p)-1}$ and $\mathbf{R}_{\mathbf{e}_{\Delta-K-L:\Delta}}^{(p)-1}$ are the noise and data covariance matrices.

D. Simulation results:

In this section, we will illustrate the proposed idea by simulation results. We will compare the MMSE PTEQ approach with the MMSE TEQ approach in an uncoded MIMO OFDM system based on exact knowledge of the channel and the noise statistics at the receiver. We consider the same OFDM parameters as in IEEE 802.11a and HIPERLAN/2, i.e., $N = 64$ and $G = 16$. We assume i.i.d. channel taps and an exponentially decaying average power delay profile with a 20-dB difference in average power between the first and last channel tap. Finally, we consider QPSK data symbols. We further consider a Rayleigh fading MIMO channel with order L and investigate the performance for different channel orders L . For each channel order L , the equalizer order is set to $K = L - G$.

Fig. 2 and Fig. 3 show the BER performance versus the average received SNR per receive antenna for $(L_T, L_R) = (2, 2)$ and $(L_T, L_R) = (2, 3)$, respectively, in a random channel adopting a synchronization delay of $\Delta = K$. The results are obtained from 500 trials, where in each trial, 100 OFDM symbols are transmitted. For each trial, we generate a new random channel, data, and noise realization. Figs. 4 and 5 show the BER performance versus the synchronization delay Δ for $(L_T, L_R) = (2, 2)$ and $(L_T, L_R) = (2, 3)$, respectively, in a fixed channel adopting a received SNR per receive antenna of 15 dB.

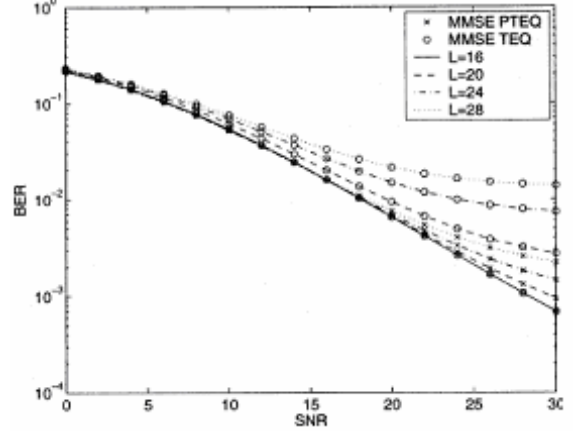


Fig. 2. Average BER versus average received SNR per receive antenna for $(L_T, L_R) = (2, 2)$ in a random channel (synchronization delay $\Delta = K$).

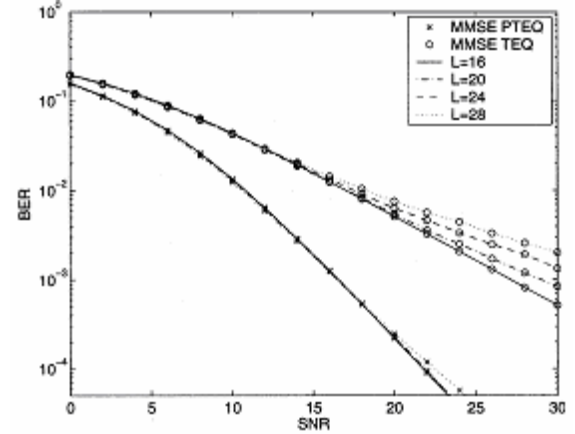


Fig. 3. Average BER versus average received SNR per receive antenna for $(L_T, L_R) = (2, 3)$ in a random channel (synchronization delay $\Delta = K$).

The results are obtained from a single trial, where 5000 OFDM symbols are transmitted. When $L_R = L_T$, we observe that the MMSE PTEQ approach and MMSE TEQ approach perform exactly the same for $L = G = 16$, whereas the MMSE PTEQ approach performs better than the MMSE TEQ approach when $L > G$. When $L_R > L_T$, we observe that the MMSE PTEQ approach performs much better than the MMSE TEQ approach, even when $L = G = 16$. Hence, the performance advantage of the MMSE PTEQ approach over the MMSE TEQ approach is much higher in MIMO OFDM systems with $L_R > L_T$ than in MIMO OFDM systems with $L_R = L_T$ (such as in SISO OFDM systems). We also see that the performance of both approaches decreases with the channel order L and that the rate of decrease is larger for $L_R = L_T$ than for $L_R > L_T$. Finally, from Figs. 4 and 5, we observe that the MMSE PTEQ approach is less sensitive to the choice of the synchronization delay than the MMSE TEQ approach.

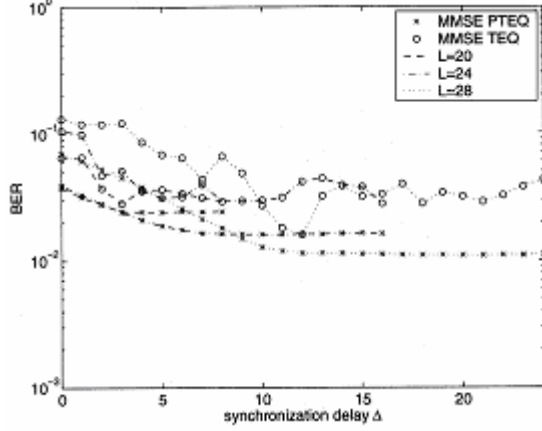


Fig. 4. BER versus synchronization delay Δ for in a fixed channel (received SNR per receive antenna 15 dB). $(L_T, L_R) = (2, 2)$

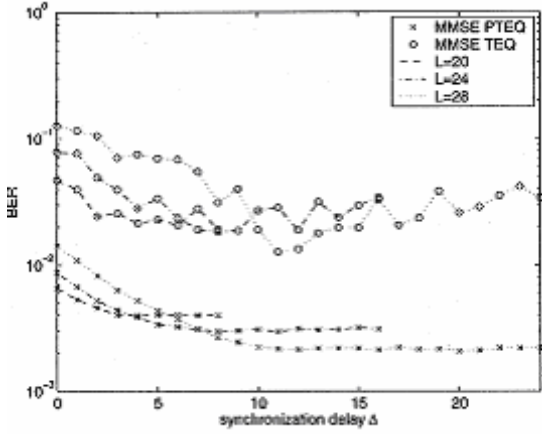


Fig. 5. BER versus synchronization delay Δ for in a fixed channel (received SNR per receive antenna 15 dB). $(L_T, L_R) = (2, 3)$

III. Signal Model for MIMO OFDM Systems in time domain:

This signal model will be used in two proceeding sections and is different to the one in per-tone equalization because the latter was aimed to be used in frequency domain. Turbo equalization can be used in both frequency and time domain but the one discussed in section V is held in the time domain.

First we should represent the mathematical model of an MIMO OFDM signal on which the equalizers will be based. Fig. 6 shows a block diagram of an OFDM transmitter with two data stream.

Let us assume that the transmitter uses L_T antennas. The transmitted signal at the i -th symbol of the l_T -th stream with $iT_S \leq t < (i+1)T_S$ can be modeled as:

$$s_{l_T, i}(t) = \sum_{n=0}^{N-1} z_{l_T, i, n} e^{j2\pi n \Delta f (t - iT_S - IT_G)}$$

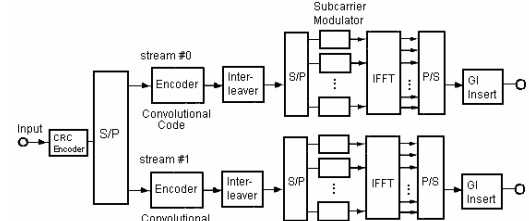


Fig. 6. Configuration of MIMO OFDM transmitter.

Where $z_{l_T, i, n}$ is the modulation signal of the l_T -th stream at the n -th subcarrier, N is the number of subcarriers and T_G is the GI duration. Sampling $s_{l_T, i}(t)$, with period $\Delta t = T_F / N$, the $N_S \times 1$ signal vector $\mathbf{s}_{l_T, i}$ can be obtained and expressed as:

$$\begin{aligned} \mathbf{s}_{l_T, i} &= [s_{l_T, i, 0}, s_{l_T, i, 1}, \dots, s_{l_T, i, N_S-1}]^T \\ &= \mathbf{F}_0 \mathbf{z}_{l_T, i} \\ (\mathbf{F}_0)_{p, q} &= e^{j\frac{2\pi}{N} q(p-G)} \\ \mathbf{z}_{l_T, i} &= [z_{l_T, i, 0}, z_{l_T, i, 1}, \dots, z_{l_T, i, N-1}]^T \end{aligned}$$

In which $T_F = 1/\Delta f$ is the FFT duration, \mathbf{F}_0 is the $N_S \times N$ IFFT matrix with $(\mathbf{F}_0)_{p, q}$ as its (p, q) -th element and $\mathbf{z}_{l_T, i}$ is the $N \times 1$ modulation signal vector of l_T -th stream. It can be easily shown that $N_S = N + G$ where $G = T_G / \Delta f$.

If the receiver employs the L_R -branch antenna diversity reception, we define an $L_R N_S \times 1$ received signal vector \mathbf{r}_i as:

$$\begin{aligned} \mathbf{r}_i &= [\mathbf{r}_{i, 0}^T, \mathbf{r}_{i, 1}^T, \dots, \mathbf{r}_{i, N_S-1}^T]^T \\ \mathbf{r}_{i, k} &= [r_{0, i, k}, r_{1, i, k}, \dots, r_{L_R-1, i, k}]^T \end{aligned}$$

in which $\mathbf{r}_{i, k}$ is an $L \times 1$ vector derived from samples of the received signals as it is shown in Fig. 7.

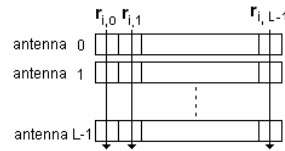


Fig. 7. Forming vectors $\mathbf{r}_{i, k}$ from received sequences.

IV. Time-Domain Equalization Using Second-Order Statistics

A. Main Concept:

One of the main approaches of time domain equalization is channel shortening in which an equalizer is first inserted to reduce the MIMO channels to ones with channel length shorter than or equal to the CP length where residual ICI and ISI are introduced and thus limit the performance. The general signal detection algorithm for MIMO-OFDM systems [6] is then applied. Moreover, this technique is sensitive to parameters including the channel shortening equalizer length and the delay [8,10]. Also unfortunately, both algorithms involve estimation of the channel matrix which requires channel length estimation followed by channel coefficient estimation. In general, channel length is estimated using information theoretic criteria such as Akaike's Information Criterion (AIC) or Minimum Description Length (MDL) which are highly complex and computationally intensive. In addition, accurate channel length estimation is difficult to achieve in practice and estimation error usually occurs, which will degrade the system performance. As for channel coefficient estimation, it is obvious that at least $(1+D)N_s$ pilot symbols are required in which D is the maximum channel length. The number of pilot symbols required increases linearly with the channel length, thereby reducing the transmission efficiency when the channel length is large.

One approach to overcome the discussed problems is to use second order statistics of the received OFDM symbols which are shifted within the CP length. This technique has been proposed by *Shaodan Ma* and *Tung-Sang Ng* [11] and is explained in details.

In this system model i -th received OFDM block is left shifted by J samples; it has certain structural properties that enable an equalizer to be designed to cancel most of ISI using SOS of the received signals. At the output of the equalizer, only two paths of the transmitted signals are retained and the signals can readily be detected.

B. Channel Model:

If we denote the frequency selective channel between the l_T -th transmit antenna/user and the l_R -th receive antenna as $h_{l_T l_R}(l)$, which is modeled as an $D_{l_T l_R}$ -th-order FIR filter. Here, the maximum channel length is defined as $D = \max_{1 \leq l_T \leq L_T, 1 \leq l_R \leq L_R} (D_{l_T l_R})$. Without loss of generality, it is assumed to satisfy $D < N - G$ which implies that the number of subcarriers is larger than the channel length plus the CP length. The i -th received block at the l_R -th receive antenna is, therefore:

$$r_i[n] = \sum_{l_T=1}^{L_T} \sum_{d=0}^D h_{l_T}(d) s_{i,l_T}[n-d] + n_i[n], n = 0, 1, \dots, N_s - 1$$

Now let following system model in which the i -th received OFDM block is left shifted by J samples as:

$$\mathbf{r}_i^{(J)} = [\mathbf{r}_i[-J]^T \ \mathbf{r}_i[-J+1]^T \ \dots \ \mathbf{r}_i[N_s-1-J]^T]^T$$

$$J = 0, \pm 1, \pm 2, \dots$$

It is apparent that $\mathbf{r}_i^{(J)}$ contains the information from two consecutive received OFDM blocks and

$$\mathbf{r}_i^{(J)} = \sum_{l_T=0}^{L_T-1} \mathbf{H}_{l_T} \mathbf{x}_{i,l_T}^{(J)} + \mathbf{n}_i^{(J)} \quad J = 0, \pm 1, \pm 2, \dots$$

in which

$$\mathbf{H}_{l_T} = \begin{bmatrix} \mathbf{h}_{l_T}(D) & \mathbf{h}_{l_T}(D-1) & \dots & \mathbf{h}_{l_T}(0) & 0 & \dots & 0 \\ 0 & \mathbf{h}_{l_T}(D) & \mathbf{h}_{l_T}(D-1) & \dots & \mathbf{h}_{l_T}(0) & \ddots & 0 \\ \vdots & \ddots & \ddots & \ddots & \ddots & \ddots & \vdots \\ 0 & \dots & 0 & \mathbf{h}_{l_T}(D) & \mathbf{h}_{l_T}(D-1) & \dots & \mathbf{h}_{l_T}(0) \end{bmatrix}$$

$$\mathbf{x}_{i,l_T}^{(J)} = [s_{i,l_T}[-D-J] \ \dots \ s_{i,l_T}[0] \ \dots \ s_{i,l_T}[N_s-1-J]]^T$$

$$\mathbf{n}_i^{(J)} = [\mathbf{n}_i[-J]^T \ \mathbf{n}_i[-J+1]^T \ \dots \ \mathbf{n}_i[N_s-1-J]^T]^T$$

Defining

$$\mathbf{H} = [\mathbf{H}_1 \ \mathbf{H}_2 \ \dots \ \mathbf{H}_{L_T}]$$

$$\mathbf{x}_i^{(J)} = \left[\left(\mathbf{x}_{i,1}^{(J)} \right)^T \ \left(\mathbf{x}_{i,2}^{(J)} \right)^T \ \dots \ \left(\mathbf{x}_{i,L_T}^{(J)} \right)^T \right]^T$$

the received signal vector $\mathbf{r}_i^{(J)}$ can be written as

$$\mathbf{r}_i^{(J)} = \mathbf{H} \mathbf{x}_i^{(J)} + \mathbf{n}_i^{(J)}, \quad J = 0, \pm 1, \pm 2, \dots$$

When $0 \leq J \leq N - D$, the signal vector $\mathbf{x}_{i,l_T}^{(J)}$ can be expressed as

$$\mathbf{x}_{i,l_T}^{(J)} = \mathbf{F}_{2N}^{(J)} \mathbf{c}_{i,l_T}, \quad l_T \in \{0, 1, \dots, L_T - 1\}, \quad 0 \leq J \leq N - D$$

where $\mathbf{c}_{i,l_T} = [\beta_{i-1,l_T}^T \ \beta_{i,l_T}^T]^T$ and

$$\mathbf{F}_{2N}^{(J)} = \begin{bmatrix} \mathbf{F}_0(N_s - D - J + 1 : N_s) & \mathbf{0} \\ \mathbf{0} & \mathbf{F}_0(N + 1 : N_s) \\ \mathbf{0} & \mathbf{F}_0(1 : N_s - J) \end{bmatrix}$$

$\mathbf{F}_0(a:b)$ denotes a submatrix of \mathbf{F}_0 , composed by the rows between the a -th row and the b -th row of \mathbf{F}_0 . So the transmit signal vector $\mathbf{x}_i^{(J)}$ can be written as

$$\mathbf{x}_i^{(J)} = \overline{\mathbf{F}}^{(J)} \mathbf{c}_i, \quad 0 \leq J \leq N - L$$

in which

$$\overline{\mathbf{F}}^{(J)} = \begin{bmatrix} \mathbf{F}_{2N}^{(J)} & \mathbf{0} & \mathbf{0} & \mathbf{0} \\ \mathbf{0} & \mathbf{F}_{2N}^{(J)} & \mathbf{0} & \mathbf{0} \\ \mathbf{0} & \mathbf{0} & \ddots & \mathbf{0} \\ \mathbf{0} & \mathbf{0} & \mathbf{0} & \mathbf{F}_{2N}^{(J)} \end{bmatrix}$$

$$\mathbf{c}_i = [\mathbf{c}_{i,1}^T \ \mathbf{c}_{i,2}^T \ \dots \ \mathbf{c}_{i,L_T}^T]^T$$

Therefore, the received signal vector $\mathbf{r}_i^{(J)}$ can be remodeled as:

$$\mathbf{r}_i^{(J)} = \mathbf{H} \overline{\mathbf{F}}^{(J)} \mathbf{c}_i + \mathbf{n}_i^{(J)}, \quad 0 \leq J \leq N - D.$$

Based on the recent system model, an equalizer can be designed to cancel most of the ISI before signal detection.

C. Time Domain Signal Detection

In this section, a time-domain signal detection algorithm based on SOS is introduced for MIMO-OFDM systems over frequency selective fading channels. Following general assumptions are made in this method:

C1) Signals from different transmit antennas/users are statistically independent, and signals from each transmit antenna/user at different subcarriers are independent with zero mean and unit variance.

C2) The noise components are independently identically distributed (i.i.d.) and independent of the signals from all transmit antennas/users.

C3) The matrix \mathbf{H} is of full column rank after removing all-zero columns, which means the nonzero columns are independent. This is a sufficient condition for detecting the signals based on SOS [12]. In order to meet this condition, the number of receive antennas, M , must be chosen to satisfy $M \geq (L + N_s)P / N_s$, so that there are more rows than columns. In most cases, when the number of receive antennas is chosen equal to the number of transmit antennas/users plus one, the above inequality will be satisfied.

C.A. Zero-Noise Case

In the absence of noise, $\mathbf{r}_i^{(J)}$ can be expressed as

$$\mathbf{r}_i^{(J)} = \mathbf{H}\mathbf{x}_i^{(J)}, \quad J = 0, \pm 1, \pm 2, \dots$$

When $0 \leq J \leq N - D$, $\mathbf{r}_i^{(J)}$ can also be modeled as

$$\mathbf{r}_i^{(J)} = \mathbf{H}\mathbf{F}^{(J)}\mathbf{c}_i, \quad 0 \leq J \leq N - D.$$

1) Equalization and Signal Detection: It is apparent that the received signal vector $\mathbf{r}_i^{(J)}$ includes $(N_s + D)$ path signals (each path signal refers to one sample signal) from each transmit antenna/user.

Defining

$$\mathbf{R}_r^{(J)} = E\{\mathbf{r}_i^{(J)}\mathbf{r}_i^{(J)*}\}$$

the equalizer is constructed based on SOS as

$$\mathbf{E} = \left(\mathbf{R}_r^{(0)} - \mathbf{R}_r^{(1)} \right) \mathbf{R}_r^{(G)\#},$$

in $(\cdot)^\#$ which represents pseudo-inverse.

This equalizer has an interesting property which we will see in proceeding. Applying this equalizer to the received signal vector $\mathbf{r}_i^{(J)}$ to yield

$$\mathbf{o}_i^{(J)} = \mathbf{E}\mathbf{r}_i^{(J)} = \mathbf{H}_{part}\mathbf{x}_{i,part}^{(J)}$$

where

$$\begin{aligned} \mathbf{H}_{part} &= [\mathbf{H}_1(N+D+1) \quad \mathbf{H}_1(D+1) \quad \dots \\ &\quad \dots \quad \mathbf{H}_p(N+D+1) \quad \mathbf{H}_p(D+1)] \\ \mathbf{x}_{i,part}^{(J)} &= [s_{i,0}[-J] \quad s_{i,0}[N-J] \quad \dots \\ &\quad \dots \quad s_{i,L_T-1}[-J] \quad s_{i,L_T-1}[N-J]]^T. \end{aligned}$$

It is apparent that most of the ISI are cancelled by the equalizer \mathbf{E} . The equalizer output $\mathbf{o}_i^{(J)}$ only contains two paths of the transmitted signals from each transmit antenna/user, i.e., $s_{i,l_T}[-J]$ and $s_{i,l_T}[N-J]$, $l_T \in \{0, 1, \dots, L_T - 1\}$. In other words, only $2L_T$ columns of the channel matrix \mathbf{H} are retained. Note that channel length information is not needed in this step.

When the matrix \mathbf{H}_{part} which contains only $2L_T$ columns of the channel matrix is known, $\mathbf{x}_{i,part}^{(J)}$ can be easily detected from the equalizer output based on the least-squares criteria [10]

$$\mathbf{x}_{i,part}^{(J)} = \left(\mathbf{H}_{part}^* \mathbf{H}_{part} \right)^\# \mathbf{H}_{part}^* \mathbf{o}_i^{(J)}, \quad J = 0, \pm 1, \pm 2, \dots$$

It is clear for example, by setting the parameter $J = -G + 1, -G + 2, \dots, N - G$, the estimation of the transmitted signal

$$\hat{s}_{i,l_T}[n], \quad l_T \in \{0, 1, \dots, L_T - 1\},$$

$n \in \{N + G - 1, N + G - 2, \dots, G\}$, are obtained from the path $s_{i,l_T}[N - J]$ of the vector $\mathbf{x}_{i,part}^{(J)}$.

2) \mathbf{H}_{part} Estimation: In order to perform signal detection, knowledge of the $L_R N_s \times 2L_T$ matrix \mathbf{H}_{part} is necessary.

For better performance, pilot symbols will be used. Note that the channel length information is not needed for the selection of pilot symbols as it is now embedded in the matrix \mathbf{H}_{part} after equalization. Suppose the pilot symbols are inserted into each transmit antenna/user's signal and \mathbf{X}_{pilot} consists of the pilot symbols, i.e.

$$\begin{aligned} \mathbf{X}_{pilot} &= [\mathbf{x}_{i_1,part}^{(J_1)} \quad \mathbf{x}_{i_2,part}^{(J_2)} \quad \dots \quad \mathbf{x}_{i_K,part}^{(J_K)}] \\ &\quad J_1, J_2, \dots, J_K = 0, \pm 1, \pm 2, \dots \end{aligned}$$

The matrix \mathbf{H}_{part} can be estimated from the equalizer output [15] as:

$$\hat{\mathbf{H}}_{part} = \mathbf{O}_{pilot} \mathbf{X}_{pilot}^* \left(\mathbf{X}_{pilot} \mathbf{X}_{pilot}^* \right)^{-1}$$

where

$$\mathbf{O}_{pilot} = [\mathbf{o}_{i_1}^{(J_1)} \quad \mathbf{o}_{i_2}^{(J_2)} \quad \dots \quad \mathbf{o}_{i_K}^{(J_K)}]$$

Albeit, In order to achieve a unique estimate of \mathbf{H}_{part} , some conditions on pilot symbols for identifiably need to be satisfied which discussion about them is avoided here.

3) Remark: In the algorithms [13], [14], knowledge of the channel matrix \mathbf{H} is necessary. Due to the structure of \mathbf{H} , only the channel coefficients $\mathbf{h}_{l_T}(0), \mathbf{h}_{l_T}(1), \dots, \mathbf{h}_{l_T}(D)$,

$l_T \in \{1, 2, \dots, L_T\}$ are required to be estimated. Since they are directly estimated from the received signal which contains $(D+1)$ paths of the transmitted signals from each transmit antenna/user, the minimum number of pilot symbols required is, therefore, $(1+D)L_T$ and linearly increases with the channel length. Also, channel length estimation is necessary before selecting the pilot symbols. On the other hand, in the proposed algorithm, only knowledge of the matrix \mathbf{H}_{part} which includes $2L_T$ columns of the channel matrix \mathbf{H} is required. Each pair of columns of the matrix, corresponding to the l_T -th transmit antenna/user, contains all the channel coefficients $(\mathbf{h}_{l_T}(0), \mathbf{h}_{l_T}(1), \dots, \mathbf{h}_{l_T}(D))$. When \mathbf{H}_{part} is estimated, it follows that the channel matrix \mathbf{H} is effectively estimated. In this case, only $4L_T$ pilot symbols are required. As aforementioned, computationally intensive channel length estimation is not needed and the transmitted signals are detected straightforwardly without the need to reconstruct the estimated channel matrix.

C.B. Channel Noise Consideration

In the presence of noise, when $0 \leq J \leq N - D$, the autocorrelation matrix of $\mathbf{r}_i^{(J)}$ is

$$\begin{aligned} \mathbf{R}_r^{(J)} &= E\{\mathbf{r}_i^{(J)}\mathbf{r}_i^{(J)*}\} = \mathbf{H}\mathbf{F}^{(J)}\overline{\mathbf{F}}^{(J)*}\mathbf{H}^* + \\ &\quad \sigma^2 \mathbf{I}_{L_R N_s}. \end{aligned}$$

If σ^2 is known, the noise contribution can be subtracted from $\mathbf{R}_r^{(0)}$, $\mathbf{R}_r^{(1)}$, $\mathbf{R}_r^{(G)}$, and, therefore, it has no impact on the equalizer which can be constructed as:

$$\begin{aligned} \mathbf{G} &= \left(\left(\mathbf{R}_r^{(0)} - \sigma^2 \mathbf{I}_{L_R N_s} \right) - \left(\mathbf{R}_r^{(1)} - \sigma^2 \mathbf{I}_{L_R N_s} \right) \right) \\ &\quad \times \left(\mathbf{R}_r^{(G)} - \sigma^2 \mathbf{I}_{L_R N_s} \right)^\# \end{aligned}$$

the output of the equalizer $\mathbf{o}_i^{(J)}$ becomes:

$$\mathbf{o}_i^{(j)} = \mathbf{E}\mathbf{r}_i^{(j)} = \mathbf{H}_{part} \mathbf{x}_{i,part}^{(j)} + \mathbf{E}\mathbf{n}_i^{(j)}$$

Taking into account the noise contribution $\mathbf{E}\mathbf{w}_i^{(j)}$ in $\mathbf{o}_i^{(j)}$, the matrix \mathbf{H}_{part} and the signal vector $\mathbf{x}_{i,part}^{(j)}$ can be detected based on the minimum mean square error (MMSE) criterion [15].

If σ^2 is unknown, it can be estimated from the singular value decomposition of $\mathbf{R}_r^{(G)}$ [16] where $\mathbf{R}_r^{(G)} = \mathbf{H}\mathbf{H}^* + \sigma^2 \mathbf{I}_{MN_r}$. Since some error generally exists in the estimation of σ^2 and this error will degrade the performance, it is generally preferred not to subtract the noise contribution from $\mathbf{R}_r^{(0)}$, $\mathbf{R}_r^{(1)}$, $\mathbf{R}_r^{(G)}$. Instead, the equalizer \mathbf{E} is constructed based on $\mathbf{E} = (\mathbf{R}_r^{(0)} - \mathbf{R}_r^{(1)})\mathbf{R}_r^{(G)\#}$ as if it were noiseless. It follows that the equalizer \mathbf{E} includes two parts: the effective equalizer and the noise contribution to the equalizer. The output of the equalizer $\mathbf{o}_i^{(j)}$ is, therefore

$$\begin{aligned} \mathbf{o}_i^{(j)} &= (\mathbf{E}_{effect} + \mathbf{E}_{noise})\mathbf{r}_i^{(j)} \\ &= \mathbf{H}_{part} \mathbf{x}_{i,part}^{(j)} + (\mathbf{E}_{effect} \mathbf{n}_i^{(j)} + \mathbf{E}_{noise} \mathbf{r}_i^{(j)}) \end{aligned}$$

last term is considered as the noise contribution to $\mathbf{o}_i^{(j)}$. As the noise contribution is not known, \mathbf{H}_{part} estimation and signal detection will be performed based on the least-squares criteria in the simulation in next section. Results will show that this algorithm performs well in the noisy case.

D. Simulation Results:

In this section, the performance of the explained algorithm is compared with other equalization techniques. In the following examples, a MIMO-OFDM system with $L_T = 2$ transmit antennas/users and $L_R = 3$ receive antennas (2×3 system) is considered. The OFDM parameters are selected as: $N = 64$ and $G = 16$. All transmitted signals are modulated with QPSK scheme. The channel parameters are assumed constant over 1500 blocks and two consecutive OFDM block pilots are inserted into each transmit antenna/user's signal at the beginning of every 1500 blocks for reliable estimation. The frequency selective fading channel responses are randomly generated with a Rayleigh probability distribution. The autocorrelation of the received signal vector is computed from a finite number of received signal vectors as:

$$\mathbf{R}_r^{(j)} \approx \frac{1}{N'} \sum_{i=1}^{N'} \mathbf{r}_i^{(j)} \mathbf{r}_i^{(j)*}$$

where N' is the number of OFDM block used and is selected as 1500 unless otherwise indicated.

D.A. The Case Where The Channel Length is Shorter Than or Equal to the CP Length: $D \leq G$

In this case, all subcarriers are orthogonal to each other and there is no IBI. The conventional algorithm [6] does the FFT in the receiver to transform the frequency selective channels into flat fading channels and then performs parallel signal detection on each subcarrier with P OFDM block pilots. In the MMSE algorithm [15], the channel length is overestimated by one as $\hat{D} = D + 1$ and the channel coefficients are estimated using Maximum Likelihood method with two consecutive OFDM block pilots. The BER performance of various algorithms under consideration for $D = 14 (D < G)$ and $D = 16 (D = G)$ are shown in Fig. 8 and Fig. 9, respectively. It is obvious that the

proposed algorithm performs substantially better than the conventional algorithm [6] and the MMSE algorithm [15] over the range of SNR considered.

D.B. The Case Where the Channel Length is longer Than the CP Length: $D > G$

In this case, the orthogonality between all subcarriers is destroyed and IBI occurs. Two indirect signal detection algorithms [13], [14] with exact knowledge of the channel length and coefficients, and the MMSE algorithm [15] are for comparison. Figs. 10 and 11 show the performance of various algorithms for $D = 18$ and $D = 20$, respectively.

D.C. Comparison:

To illustrate the impact of the channel length and the CP length on the explained algorithm, the performance for 14, 16, 18, 20 cases are shown in Fig. 12. It is obvious that the performance is only slightly degraded when the channel length increases from 14 ($D < G$) to 20 ($D > G$). It demonstrates that the channel and CP lengths have insignificant effect on the explained algorithm. It also verifies that this algorithm is applicable irrespective of whether the channel length is shorter than, equal to or longer than the CP length.

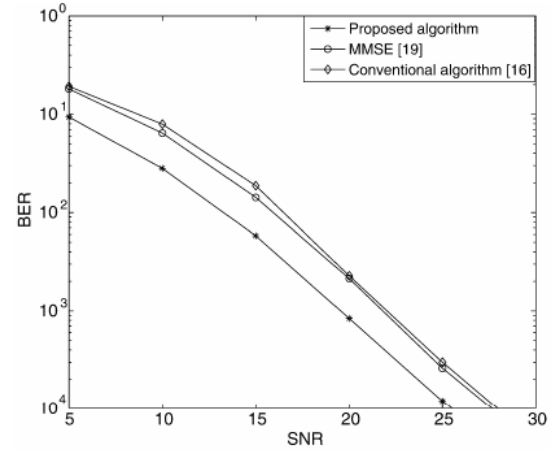


Fig. 8. The D=14 case.

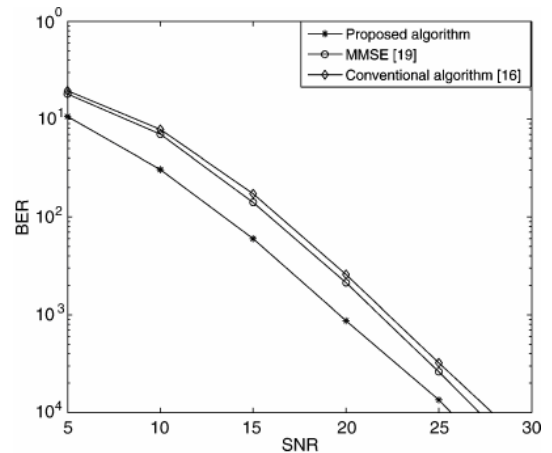


Fig. 9. The D=16 case.

E. Conclusion:

A time domain equalizer using the second-order statistics (SOS) of the received OFDM symbols which are shifted within the CP length was explained which partially cancels the ICI and ISI. It was illustrated that the channel length information is not needed and only columns of the channel matrix need to be estimated with a minimum of pilot symbols for identifiability.

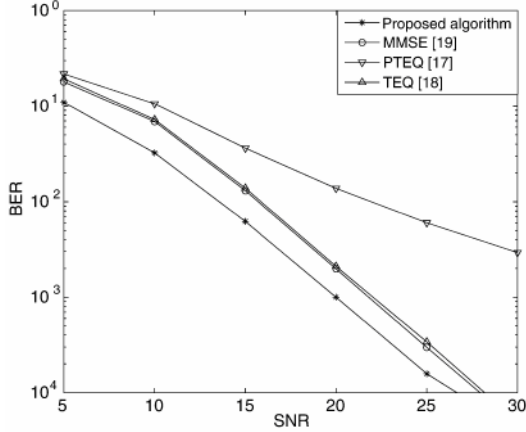


Fig. 10. The D=18 case.

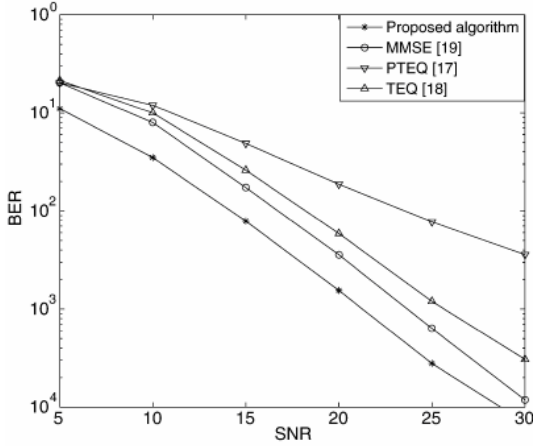


Fig. 11. The D=20 case.

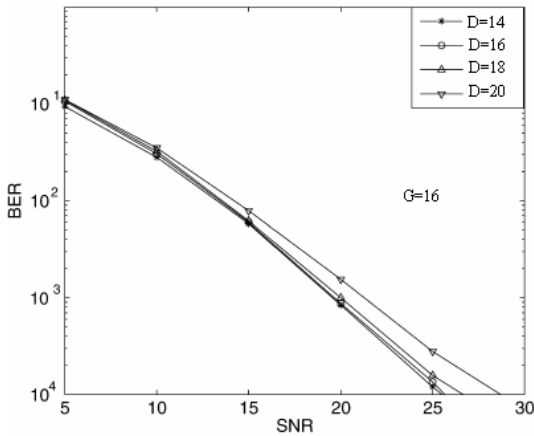


Fig. 12. SOS-based algorithm for D=14, 16, 18, 20 cases (G=16).

In addition, it has been seen that this algorithm is applicable to general MIMO-OFDM systems irrespective of whether the CP length is longer than, equal to or shorter than the channel length. Simulation results show that this algorithm outperforms the existing ones in all cases.

Interlude: Shaodan Ma and Tung-Sang Ng also proposed another algorithm [17] in which the received OFDM symbols are shifted by more than or equal to the CP length. It turns out that the SOS matrices of the shifted received OFDM symbols have different and useful structures. With these structures, a blind equalizer can be designed to completely suppress the ICI and ISI using the SOS of the shifted received OFDM symbols. Unlike first algorithm proposed by them, the equalizer output contains only one sampled signal from each transmit antenna. Consequently, only a one-tap equalizer is needed to detect the time domain signals with the aid of one pilot OFDM symbol. By computer simulations, they show that this technique performs well in both cases where the CP length is longer than/equal to or shorter than the channel length. In addition, only one parameter (the number of shifts in excess of the CP length, K) can be varied in the recent technique and simulation results show that it is robust against variation of K . This is an advantage over the time-frequency domain techniques which are sensitive to a number of parameters such as the channel shortening equalizer length and the delay.

V. Turbo Equalization:

A. Main Concept:

The basic elements of most communication systems are depicted in Fig. 13. To estimate the transmitted data optimally, in terms of minimizing the bit error rate (BER), receiver A must take into account the ECC, the interleaver, the symbol mapping, and knowledge of the channel. With so many factors involved, the resulting statistical relationship rapidly becomes difficult to manage making optimal receiver infeasible in most practical systems. Fig. 13(c) shows one of the common ways in which a practical receiver first tries to compensate the channel effects. Once the transmitted channel symbols have been estimated, they are demapped into their associated code bits, deinterleaved and then decoded using a BER optimal decoder for the ECC. The separation of equalizer and decoder can be done using hard or soft information. The remarkable performance of turbo codes makes it clear that the soft information need not only flow in one direction. As it is shown in Fig. 13(d), the error control decoding algorithm can generate its own soft information indicating the relative likelihood of each of the transmitted bits. This soft information could then be properly interleaved and taken into account in the equalization process, creating a feedback loop between the equalizer and decoder. This is the main idea of the so called "Turbo Equalizer". To avoid short cycles in the feedback and in hopes of avoiding local minima and limit cycle behavior in the process, when soft information is passed between constituent algorithms, such information is never formed based on the information passed into the algorithm concerning the same bit (channel symbol). As a result, only "extrinsic information" is passed between equalizer and decoder. The soft information can be produced in terms of log likelihood ratios. Detailed discussion on Turbo Equalization is beyond the scope of this text and can be found in [18]. Following sections present OFDM and MIMO-OFDM turbo equalization, respectively.

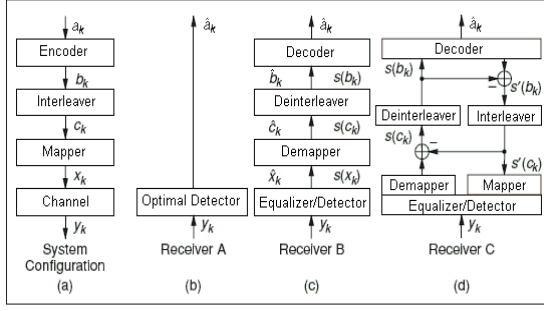


Fig. 13. System configuration and three receiver structures: the optimal detector (receiver A), one-time equalization and decoding using hard or soft decisions (receiver B), and turbo equalization (receiver C).

B. MIMO OFDM Turbo Equalization:

In this section, we will consider one of the main methods of OFDM turbo equalization presented in [20]. The proposed algorithm uses turbo equalizer just for ICI canceling but as it can be seen in later papers [19], ISI can be cancelled in the same manner. A receiver using turbo equalizer with two branch antenna diversity is depicted in Fig. 14.

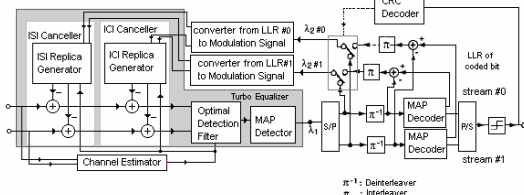


Fig. 14. Block diagram of OFDM turbo receiver.

Equalizer consists of an ICI canceller, an ISI canceller, an optimal detection filter, a MAP detector and the MAP decoder. In [20], an ISI combiner is introduced to combine the leaked signal energy spread to the next symbol as ISI. This is not necessary because this term of ISI can be considered in ISI canceller, too. First, the equalizer performs the timing recovery and the channel estimation by using the preamble of a packet. Here we assume that the timing recovery is ideal. The channel estimator employs the MMSE criterion to estimate the channel impulse response in the time domain. The turbo equalizer exploits LLR that the MAP decoder calculated in previous iteration. The iterative process continues until the number of the iterations exceeds a threshold.

To complete our signal model discussed previously, here we assume that received vector \mathbf{r}_i at i -th symbol can be written as:

$$\mathbf{r}_i = \sum_{l_T=0}^{L_T-1} (\mathbf{H}_{0,l_T} \mathbf{s}_{l_T,i} + \mathbf{H}_{-1,l_T} \mathbf{s}_{l_T,i-1}) + \mathbf{n}_i$$

where \mathbf{n}_i is the white Gaussian noise vector defined in the same

way as $\mathbf{r}_i \cdot \mathbf{H}_{0,l_T}$ and \mathbf{H}_{-1,l_T} are $L_R N_S \times N_S$ matrices respectively representing the channel impulse responses of the l_T -th stream for ICI and ISI and are defined as:

$$\mathbf{H}_{0,l_T} = \begin{bmatrix} \mathbf{h}_{l_T,0} & \mathbf{0} & \cdots & \cdots & \mathbf{0} \\ \vdots & \ddots & \ddots & \ddots & \vdots \\ \mathbf{h}_{l_T,D} & \cdots & \mathbf{h}_{l_T,0} & \ddots & \vdots \\ \mathbf{0} & \ddots & \ddots & \ddots & \mathbf{0} \\ \mathbf{0} & \mathbf{0} & \mathbf{h}_{l_T,D} & \cdots & \mathbf{h}_{l_T,0} \end{bmatrix}$$

$$\mathbf{H}_{-1,l_T} = \begin{bmatrix} \mathbf{0} & \mathbf{h}_{l_T,D} & \cdots & \mathbf{h}_{l_T,1} \\ \vdots & \ddots & \ddots & \vdots \\ \mathbf{0} & \ddots & \ddots & \mathbf{h}_{l_T,D} \\ \mathbf{0} & \ddots & \ddots & \mathbf{0} \end{bmatrix}$$

$$\mathbf{h}_{l_T,d} = [h_{l_T,0,d} \ h_{l_T,1,d} \ \cdots \ h_{l_T,L_R-1,d}]^T$$

where $\mathbf{h}_{l_T,l_R,d}$ is the complex amplitude of the d -th propagation path ($d = 0, 1, \dots, D$) between the l_T -th transmit antenna and the l_R -th receive one. $D\Delta t$ is the maximum delay difference, and it is assumed that $G \leq D \leq N_S - 1$. Using equivalent channel matrices $\mathbf{H}_{C,l_T} = \mathbf{H}_{0,l_T} \mathbf{F}_0$ and $\mathbf{H}_{S,l_T} = \mathbf{H}_{-1,l_T} \mathbf{F}_0$ for simplicity, the received signal vector \mathbf{r}_i is rewritten as:

$$\mathbf{r}_i = \mathbf{H}_C \mathbf{z}_i + \mathbf{H}_S \mathbf{z}_{i-1} + \mathbf{n}_i$$

Where \mathbf{H}_C and \mathbf{H}_S are respectively $L_R N_S \times L_T N$ equivalent channel metrics of ICI and ISI for all streams and \mathbf{z}_i is the $L_T N \times 1$ modulation signal vector for all streams. They are defined as:

$$\mathbf{H}_C = [\mathbf{H}_{C,0} \ \mathbf{H}_{C,1} \ \cdots \ \mathbf{H}_{C,L_T-1}]$$

$$\mathbf{H}_S = [\mathbf{H}_{S,0} \ \mathbf{H}_{S,1} \ \cdots \ \mathbf{H}_{S,L_T-1}]$$

$$\mathbf{z}_i = [\mathbf{z}_{i,0}^T \ \mathbf{z}_{i,1}^T \ \cdots \ \mathbf{z}_{i,L_T-1}^T]$$

In this signal model, MIMO OFDM with L_T antennas and N subcarriers is equivalent to OFDM with $L_T N$ subcarriers. We can define extended vector \mathbf{r}'_i which includes the total energy of the i -th symbol and observes ISI from $(i+1)$ -th symbol as $\mathbf{r}'_i = \mathbf{H}'_{S,1} \mathbf{z}_{i+1} + \mathbf{H}'_C \mathbf{z}_i + \mathbf{H}'_{S,-1} \mathbf{z}_{i-1} + \mathbf{n}'_i$. All prim versions of vectors and matrix have $N_S + D$ instead of N_S in their dimension. Now we begin with discussing two states of Turbo Equalizer here:

(1) Initial Processing:

In the initial processing the ISI canceller uses soft decision feedback cancellation and subtracts an ISI replica which is generated using both an estimated vector of the mean of the modulation signal at the $(i-1)$ -th symbol $\hat{\mathbf{z}}_{i-1}$ and an estimated equivalent ISI channel matrix $\hat{\mathbf{H}}_S$ as:

$$\mathbf{r}_{c,i} = \mathbf{r}_i - \hat{\mathbf{H}}_S \hat{\mathbf{z}}_{i-1}$$

Elements of $\hat{\mathbf{z}}_{i-1}$ are derived from LLRs that the MAP detector calculated at the previous symbol. For example in QPSK case, these terms can be expressed as:

$$\hat{z}_{l_T,i,n} = \frac{1}{\sqrt{2}} \tanh\left[\frac{\lambda_2(b_0)}{2}\right] + j \frac{1}{\sqrt{2}} \tanh\left[\frac{\lambda_2(b_1)}{2}\right]$$

Where $\lambda_2(b)$ is the LLR of the coded bit b .

The ICI canceller cannot operate in the initial processing because the MAP decoding has not been accomplished and LLR of the coded bits in the present symbol is not available. Thus, the equalizer suppresses ICI by using the optimal detection filter which performs linear processing on $\mathbf{r}_{c,i}$ and its output is:

$$\tilde{\mathbf{z}}_i = [\tilde{z}_{0,i,0} \tilde{z}_{0,i,1} \dots \tilde{z}_{0,i,N-1}]^T = \mathbf{G}^H \mathbf{r}_{c,i}$$

The filter estimates \mathbf{G} on the MMSE criterion as using estimated equivalent ICI channel matrix $\hat{\mathbf{H}}_C$:

$$\mathbf{G} = \hat{\mathbf{H}}_C (\hat{\mathbf{H}}_C^H \hat{\mathbf{H}}_C + \sigma_n^2 \mathbf{I}_{L_T N})^{-1}$$

σ_n^2 is an estimated noise power and $\mathbf{I}_{L_T N}$ is an $L_T N \times L_T N$ identity matrix. The process contains the Fourier transform. Finally, the MAP detector generates LLR $\lambda_1(b)$. Assuming that the output of the optimal detection filter $\tilde{\mathbf{z}}_i$ is a Gaussian process, we have:

$$\lambda_1(b_p) = \log \frac{\sum_{b_q \in Q, b_q \neq b_p, b_p=1} P(\tilde{z}_{l_T,i,n} | b_q)}{\sum_{b_q \in Q, b_q \neq b_p, b_p=0} P(\tilde{z}_{l_T,i,n} | b_q)}$$

where Q is the set of bits that determines $z_{l_T,i,n}$.

Using output LLR of the MAP detector, MAP decoder calculates the second LLR of the coded and the information bits along the trellis of the convolutional code.

(2) Iterative Processing:

If the CRC decoder detects any packet errors from LLR of the information bit, the receiver shifts from the initial processing to iterative one. In the iterative processing, the turbo equalizer does not simply suppress ISI and ICI of the target stream but cancels ISI and ICI of the target stream and the other streams - that is the co-channel interference (CCI)- in order to obtain the antenna diversity gain. By processing \mathbf{r}'_i , the turbo equalizer can exploit the total received signal energy. In this case, the ISI canceller removes the ISI components of the received signal. It generates an ISI replicas using $\hat{\mathbf{z}}_{i-1}$ and $\hat{\mathbf{z}}_{i+1}$ that are generated from LLR of the MAP decoder output.

Next, the ICI canceller for the m -th subcarrier of the l_T -th stream subtracts an ICI replica from the ISI canceller output $\mathbf{r}'_{c,i}$. The replica contains the ICI components of all the streams except the signal component for the m -th subcarrier of the l_T -th stream. Moreover, the optimal detection filter carries out the signal combining plus the Fourier transform so as to suppress the residual error of the cancellation. The turbo equalization for the m -th subcarrier of the l_T -th stream after ISI cancellation is expressed by the following equations.

(i) ICI Canceller:

$$\mathbf{r}'_{l_T,i,m} = \mathbf{r}'_{c,i} - \hat{\mathbf{H}}'_C \hat{\mathbf{z}}_{l_T,i,m}$$

where $\hat{\mathbf{z}}_{l_T,i,m}$ is as the same as $\hat{\mathbf{z}}_{l_T,i}$ with its $(l_T N + m)$ -th element equal to zero and $\hat{\mathbf{H}}'_C$ is an estimate of \mathbf{H}'_C .

(ii) Optimal Detection Filter:

$$\tilde{z}_{l_T,i,m} = \mathbf{w}_{l_T,m}^H \mathbf{r}'_{l_T,i,m}$$

$$\mathbf{w}_{l_T,m} = \frac{(\hat{\mathbf{H}}'_C)_{l_T,m}}{(\hat{\mathbf{H}}'_C)_{l_T,m}^H (\hat{\mathbf{H}}'_C)_{l_T,m} + \hat{\sigma}_{IN}^2}$$

$$\sigma_{IN}^2 = E \left[\left| \mathbf{r}_{c,i} - \hat{\mathbf{H}}'_C \hat{\mathbf{z}}_i \right|^2 \right]$$

$$\approx \left| \mathbf{r}_{c,i} - \hat{\mathbf{H}}'_C \hat{\mathbf{z}}_i \right|^2 \text{ for large } L_R(N_S + D)$$

where $(\hat{\mathbf{H}}'_C)_{l_T,m}$ is the $(l_T N + m)$ -th column vector of $\hat{\mathbf{H}}'_C$ and $\hat{\sigma}_{IN}^2$ is the estimated variance of the noise and the residual error. We have assumed that the residual error is white and not so dominant. The above process is carried out for all the subcarriers of all the streams.

The MAP detector transforms the equalized signal $\tilde{z}_{l_T,i,n}$ into LLR of the coded bit using equation:

$$\lambda_1(b_p) = \log \frac{\sum_{b_q \in Q, b_q \neq b_p, b_p=1} P(\tilde{z}_{l_T,i,n} | b_q) P(b_q)}{\sum_{b_q \in Q, b_q \neq b_p, b_p=0} P(\tilde{z}_{l_T,i,n} | b_q) P(b_q)}$$

On the assumption that the filter output is a Gaussian process $P(\tilde{z}_{l_T,i,n} | b_q)$ in the QPSK case is given by:

$$P(\tilde{z}_{l_T,i,n} | b_q) \propto e^{-\frac{|\tilde{z}_{l_T,i,n} - \frac{\mu(l_T,n)}{\sqrt{2}}(S_q + jS_i)|^2}{v^2(l_T,n)}}$$

where S_q is equal to 1, if b_q is 1 and otherwise is equal to -1.

$\mu(l_T, n)$ is the equivalent amplitude of the n -th subcarrier signal at the l_T -th stream and $v^2(l_T, n)$ is the variance of the error signal. They are given by:

$$\mu(l_T, n) = E \left[\tilde{z}_{l_T,i,n} \tilde{z}_{l_T,i,n}^* \right] = \mathbf{w}_{l_T,n}^H (\hat{\mathbf{H}}'_C)_{l_T,n}$$

$$v^2(l_T, n) = E \left[\left| \tilde{z}_{l_T,i,n} \right|^2 \right] - \mu^2(l_T, n)$$

$$= \mathbf{w}_{l_T,n}^H E \left[\mathbf{r}'_{l_T,i,m} \mathbf{r}'_{l_T,i,m}^H \right] \mathbf{w}_{l_T,n} - \mu^2(l_T, n)$$

In addition $P(b_q = 1)$ and $P(b_q = 0)$ are derived from LLR $\lambda_2(b)$ as follows:

$$P(b_q = 1) = \frac{\exp[\lambda_2(b_q)]}{1 + \exp[\lambda_2(b_q)]}$$

$$P(b_q = 0) = \frac{1}{1 + \exp[\lambda_2(b_q)]}$$

C. Simulation and Results:

This simulation results are quoted from [19] directly. Computer simulations to verify the performance of the MIMO-OFDM turbo receiver were conducted following an extended specification of 5-GHz wireless LAN. The simulation conditions are listed in table below:

| Antenna L_T, L_R | 2 |
|-----------------------|----------------------------------|
| Modulation | QPSK, 16QAM |
| Transmission rate | 24, 48 Mbit/s |
| FFT point | 64 |
| Active subcarrier | 52 (pilot: 4, data: 48) |
| GI duration | 0.8 μ s (16 pt) |
| Symbol duration | 4.0 μ s (80 pt) |
| Data in a packet | 240 Byte (10-symbol in 16QAM) |
| Channel coding | R=1/2, K=7, convolutional code |
| MAP decoder | Max-Log-MAP algorithm |
| Channel model | 18-path with exponential decay |
| Maximum delay | 1.7 μ s (34 pt) |
| Maximum Doppler freq. | 0Hz |

The numbers of antennas, L_T and L_R , were set equal to two.

The convolutional code with the constrained length $K = 7$ and the code rate $R = 1/2$ was assumed as the channel coding. Interleaving was carried out symbol by symbol and along the bit sequence for the subcarriers in one symbol. The channel model was assumed to be 18-path Rayleigh fading with the average power of each path decaying exponentially. The delay components were located at every 2 pt, where pt denotes $\Delta t = 50$ ns. Thus, the maximum delay difference was equal to 1.7 μ s (34 pt), and the RMS delay spread became 330 ns. The power ratio ρ_D of the first path to the last one was set equal to 20 dB and the maximum Doppler frequency f_D was 0Hz.

Note that the channel model we used is appropriate for the simulations even although it is sample-spaced one and is different from the standardized model for the 5-GHz wireless LAN, which is a fractionally spaced one. This is because it has the same number of paths as the standardized model, a maximum delay differences almost the same as 1.76 μ s maximum delay difference of the standardized model, and fluctuation of the delay spread. Another reason for using the channel model is avoiding the fractional sampling.

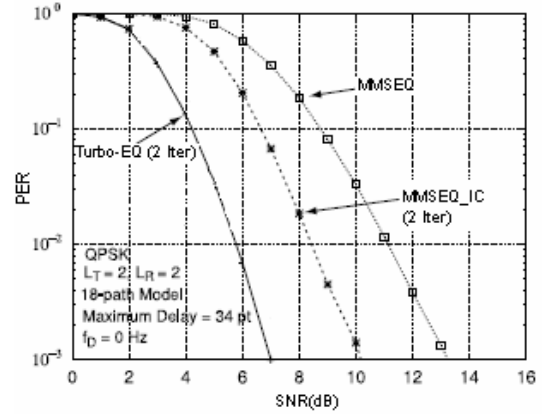
The channel estimation method of the RLS algorithm uses the two-symbol-long preamble for estimating the channel impulse responses [21]. It was also assumed that the timing recovery is ideal and that the exact noise power is known at the receiver. The receiver can anyway estimate the noise power from the mean error of the RLS algorithm.

For comparison, some simulation results of MMSED and the MMSE detector with the iterative interference canceller (MMSED-IC) in the post-FFT processing are also plotted [22], [23]. MMSED-IC carries out MMSED in the initial processing and cancels CCI by using LLR in the iterative processing so as to obtain the antenna diversity gain.

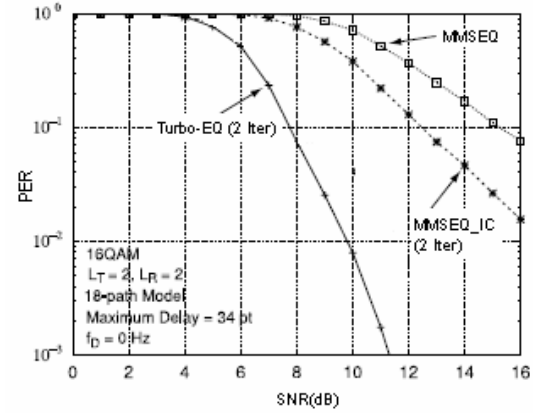
Figure 15 shows the PER performance of QPSK and 16QAM. The iteration of the turbo equalization denoted by "iter." is equal to 2. It is seen that the performance of the conventional MMSED is severely degrade by ISI and ICI, and that MMSED-IC can reduce CCI from the spatially multiplexed signals by subtracting a replica of the other stream from the received signal. The degradation of the MMSED-IC performance, however, cannot be neglected. Turbo-EQ, in contrast, can achieve a good performance by eliminating both ISI and ICI besides CCI, and can improve 7.6 dB and 5 dB in the average E_b/N_0 to achieve PER of 10^{-1} for 16QAM in comparison with MMSED and MMSED-IC, respectively.

The degradation of the simplified turbo equalizer, which uses MMSED-ISIC as the initial processing, can be neglected in the QPSK case but amounts to about 1 dB in the 16QAM case. This is because ICI damages MMSED-ISIC with 16QAM more than it damages MMSED-ISIC with QPSK, and the successive iterative processing therefore cannot improve PER.

The delay spread performance with an average E_b/N_0 of 10 dB is shown in Fig. 16 16QAM was assumed as the modulation scheme and the delay spread was adjusted by



(a) QPSK



(b) 16QAM

Fig. 15. Packet error rate performance

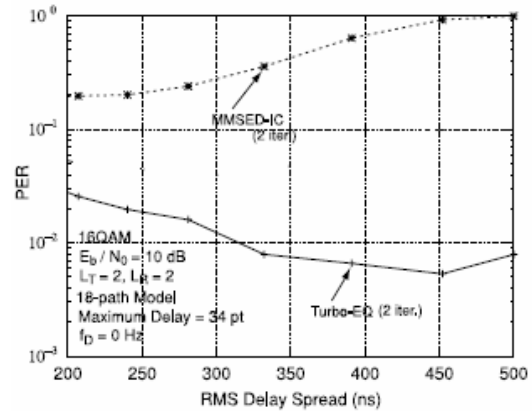


Fig. 16 Delay spread performance

changing the power ratio ρ_D . The maximum delay was 1.7 μ s. The PER performances of MMSED-IC and the simplified turbo equalizer deteriorate as the delay spread increases because then ICI and ISI increase

Up to the delay spread of 450 ns, however, the turbo equalizer can improve the PER performance by obtaining the frequency diversity gain with the channel coding. Since MMSED-ISIC of the simplified turbo equalizer cannot sufficiently suppress ICI, the simplified turbo equalizer is more damaged by large delay components.

D. Conclusion:

Here we have discussed a MIMO OFDM turbo receiver suitable for multipath fading channels in which the delay difference is greater than GI. This equalizer consists of ISI and ICI cancellers, an optimal filter, a MAP detector and MAP decoders. It can cope with both ISI and ICI by iterating the MIMO OFDM turbo equalization and the MAP decoding. Computer simulations which were quoted from [19], show that this receiver can maintain good performances in multipath environments even when the maximum delay is greater than GI and the delay spread is large. With 16QAM, turbo receiver can gain the average E_b / N_0 of 7.6 dB and 5 dB at PER of 10^{-1} in comparison with respectively the conventional MMSE detector and the MMSE detector with the iterative interference canceller in the post-FFT processing,

References

- [1] G. Leus and M. Moonen, "Per-Tone Equalization for MIMO OFDM Systems," IEEE Trans. on Sig. Proc., Vol. 51, No. 11, Nov 2003.
- [2] K. Van Acker, G. Leus, and M. Moonen. "Per Tone Equalization for DMT Based Systems," IEEE Trans. on Commun., 49(1):109–119, January 2001.
- [3] N. Al-Dhahir and J. M. Cioffi. "Optimum Finite-Length Equalization for Multicarrier Transceivers," IEEE Trans. on Commun., 44(1):56–64, January 1996.
- [4] E. Karami and M. Juntti, "Equalization of MIMO-OFDM Channels Using Bussgang Algorithm," Centre for Wireless Communications (CWC), University of Oulu, P.O. Box 4500, FIN-90014, Oulu, Finland.
- [5] A. Maleki-Tehrani, B. Hassibi, and J. M. Cioffi, "Adaptive equalization of multiple-input multiple-output frequency selective channels," in Proc. Asilomar Conf. Signals, Syst., Comput., Pacific Grove, CA, Oct. 1999, pp. 547–551.
- [6] A. van Zelst and T. C. W. Schenk, "Implementation of a MIMO OFDM-based wireless LAN system," IEEE Trans. Signal Process., vol. 52, pp. 483–494, Feb. 2004.
- [7] G. Leus, M. Moonen, "Per-tone equalization for MIMO OFDM systems", IEEE Trans. Signal Processing, vol. 51, pp. 2965-2975, Nov. 2003.
- [8] P.J.W. Melsa, R.C. Younce, and C.E. Rohrs, "Impulse response shortening for discrete multitone transceivers", IEEE Trans. Commun., vol. 44, pp. 1662-1672, Dec. 1996.
- [9] N. Al-Dhahir, "FIR channel-shortening equalizer for MIMO ISI channels", IEEE Trans. Commun., vol. 49, pp. 213-218, Feb. 2001.
- [10] J. Zhang and W. Ser, "Delay Selection for TEQ in OFDM systems", IEEE International Symposium on Signal Processing and Information Technology (ISSPIT 2003), pp. 443-446, 2003.
- [11] S. D. Ma and T.S. Ng, "Time domain signal detection based on second order statistics for MIMO-OFDM systems", IEEE Trans. Signal Process., vol. 55, NO. 3, Mar. 2007.
- [12] A. Gorokhov and P. Loubaton, "Subspace-based techniques for blind separation of convolutive mixtures with temporally correlated sources," IEEE Trans. Circuits Syst. I, Fundam. Theory Appl., vol. 44, pp. 813–820, Sep. 1997.
- [13] G. Leus and M. Moonen, "Per-tone equalization for MIMO OFDM systems," IEEE Trans. Signal Process., vol. 51, pp. 2965–2975, Nov. 2003.
- [14] N. Al-Dhahir, "FIR channel-shortening equalizers for MIMO ISI channels," IEEE Trans. Commun.vol. 49, pp. 213–218, Feb. 2001.
- [15] S. M. Kay, Fundamentals of Statistical Signal Processing: Estimation Theory. Englewood Cliffs, NJ: Prentice-Hall, 1993.
- [16] J. Q. Shen and Z. Ding, "Direct blind MMSE channel equalization based on second-order statistics," IEEE Trans. Signal Process., vol. 48, pp. 1015–1022, Apr. 2000.
- [17] S. D. Ma and T.S. Ng, "Semi-blind time domain equalization for MIMO OFDM systems", Circuits and Systems, 2006. APCCAS 2006. IEEE Asia Pacific Conference on.
- [18] R. Koetter, C. Singer and M. Tuchler, "Turbo Equalization", IEEE Signal Process. Mag., vol. 21, no. 1, pp. 67-80, Jan. 2004.
- [19] S. Suyama, H. Suzuki and K. Fukawa, "A MIMO OFDM receiver employing the low-complexity Turbo Equalization in multipath environments with delay difference greater than guard interval", IEICE Trans. Commun., vol.E88-B, no. 1; Jan. 2005.
- [20] S. Suyama, H. Suzuki and K. Fukawa, "An OFDM receiver employing Turbo Equalization for multipath environments with delay difference greater than guard interval", 57th IEEE semiannual, vol. 1; Apr. 2003.
- [21] K. Fukawa, H. Suzuki, and T. Usami, "OFDM channel estimation with RLS algorithm for different pilot schemes in mobile radio transmission," IEICE Trans. Commun., vol.E86-B, no.1, pp.266–274, Jan. 2003.
- [22] S. Kurosaki, Y. Asai, T. Sugiyama, and M. Umehira, "SDM COFDM scheme using feed-forward inter channel interference canceller for broadband mobile communications" IEEE Veh. Technol. Conf., pp.1079– 1083, May 2002.
- [23] Y. Li, J.H. Winters, and N.R. Sollenberger, "MIMO-OFDM for wireless communications: Signal detection with enhanced channel estimation," IEEE Trans. Commun., vol.50, no.9, pp.1471–1477, Sept. 2002.

